AN EXPLANATION FOR THE UNEXPECTED INTERACTIONS OF SILICA NANOPARTICLES USING THE SOFT PARTICLE MODEL

Shuying Chen[1], Kevin Brown[2], and Mark Jermy[1]

[1] Department of Mechanical Engineering, University of Canterbury, Christchurch 8041, New Zealand

[2] GEOKEM, P.O. Box 30-125, Barrington, Christchurch, New Zealand

jasonchen1212@hotmail.com

Keywords: *Colloidal silica, soft particle, silica chemistry, aggregation, silica scaling, amorphous silica deposition.*

ABSTRACT

Under geothermal conditions, silica scaling is essentially the deposition of colloidal silica: when cooled geothermal brine is reinjected, monomeric (dissolved) silica will polymerise and form silica nanoparticles. These will transport and deposit on the mineral surfaces, and may eventually block the fluid pathways in the aquifer.

Silica deposition in geothermal reinjection may be treated as a two-step process: the first step is the initial attachment between silica particles and "clean" mineral surfaces on which no (monomeric or polymerised) silica has already deposited, and the other is the later attachment between suspended and previously deposited particles. If it is assumed that the initial attachment is instantaneous, and the deposition rate is controlled by the later attachment, which is essentially an aggregation problem.

It has been shown that DLVO theory can predict the stability of colloids for certain chemical compositions with reasonable accuracy. However, amorphous silica particle is an exception. To understand this, a hypothesis has been proposed (De Gennes 1987, Healy 1994), assuming that the unique behaviours are induced by the hairy layer (also called the gel layer) made of polymer chains of silicone anchored on the surface of the colloidal silica. Ohshima (2015) proposed a general model to quantify the electrostatic interactions caused by ion-penetrable surface layers of polyelectrolytes. The present work applies Ohshima's model to explain the experimental observations of Škvarla (2013). The resulting model provides an explanation of the non-DLVO behaviour of silica particles.

1. INTRODUCTION

Under typical geothermal conditions, silica scaling is (Brown 2011) mainly dominated by the deposition of colloidal. From the perspective of the authors of the present work, the deposition process can be described as follows: monomeric silica may firstly polymerise to form nuclei which grow to become colloidal particles, which would coat the fracture surfaces (to at least one particle thick) in a time much less than the lifetime of the well. Hence, one can treat the wall as having the electrochemical properties of silica, regardless of rock mineral content, i.e. the deposition is recognised as the interaction between deposited and suspended particles.

The interaction behaviours of silica nanoparticles under geothermal conditions decides the attachment (aggregation) rate, which consequently determines the deposition rate. Therefore, a quantitatively description of the interaction of colloidal silica is of great value to the geothermal industries in predicting the rate of formation of silica scale.

DLVO theory (Deraguin and Landau 1941, Verwey and Overbeek 1955), is commonly used to quantitatively describe the interaction between colloids. The theory describes the total interaction potential between colloidal silica particles V_T as the sum of the attractive potential V_A due to the van der Waals force and the repulsive potential V_E due to the electrostatic force:

$$V_T = V_A + V_E \tag{1}$$

For simplicity, the case of two identical colloidal particles is considered below. The attractive potential between the two colloids with the same radius a can be represented by (Hamaker 1937):

$$V_A = -\frac{A}{6}\left(\frac{2}{u^2+4u} + \frac{2}{(u+2)^2} + ln\left[\frac{u^2+4u}{(u+2)^2}\right]\right) \tag{2}$$

where, $u = H/a$ is the dimensionless surface-to-surface distance between particles, H is the separation distance (i.e. dimensional surface-to-surface distance), and A is the Hamaker constant, represented by Eq. 3 below (Hamaker 1937, London 1937):

$$A = 0.75 k_B T (1+2\kappa H) e^{-2\kappa H} + \frac{3\hbar\omega}{16\sqrt{2}} \frac{(n_1^2-n_3^2)^2}{(n_1^2+n_3^2)^{3/2}} \left[1+\left(\frac{H}{\lambda}\right)^q\right]^{-1/q} \tag{3}$$

where, k_B is the Boltzmann constant, T is the absolute temperature, $\kappa = \sqrt{\frac{2e^2 N_A c_i z^2}{\varepsilon k_B T}}$ is the Debye-Huckel parameter, e is the electron charge, N_A is Avogadro's number, c_i is the concentration of the background electrolyte, z is the valence of the electrolyte, ε is the permittivity, $\hbar$ is the Planck constant divided by 2π, $\lambda = \frac{c}{\pi^2\omega}\sqrt{\frac{2}{n_3^2(n_1^2+n_3^2)}}$ is the characteristic wavelength of the retardation effect, c is the speed of light, $\omega = 3.3 \times 10^{15}$ is the characteristic frequency of the retardation effect, $n_1 = 1.43$ and $n_2 = 1.33$ are the refractive index of silica and medium (water) respectively, and $q = 1.185$ is a fitting factor (Škvarla 2013).

The electrostatic repulsion between two similar colloids is due to the surface charge φ_0. In the case of amorphous silica, the silanol group may either dissociate a proton to the solution or obtains a proton from the solution depending on the pH. Hence, the surface of a silica particle will be either negatively or positively charged unless the pH is at the "point of zero charge" where these effects are balanced.

Ions from the background electrolyte are adsorbed to the charged surface to form a charged layer, called the Stern layer or the first layer. Due to the existence of the first layer, ions with opposite charge are attracted and electrically mask the first layer. These ions form another charged layer, called the second layer or the diffuse layer since it is loosely organized. The assembly comprising the two charged layers is named the "double layer" or "electrical double layer".

By assuming the surface potential is maintained to be constant (Derjaguin 1940), the electrostatic repulsion potential can be expressed as (Eq. 4):

$$V_E = 2\pi\varepsilon\varphi_0{}^2 r \ln[1 + \exp(-\kappa h)] \quad (4)$$

In practice, another parameter – the zeta-potential (or ζ-potential) is usually substituted in place of surface potential φ_0 in Eq. 4, which may be smaller than φ_0 in absolute value but is easier to be estimated by measuring the electrical mobility of the sols.

Theoretically, since homogenous silica nucleation is favoured under geothermal conditions (Weres et al. 1981), given sufficient time, an oversaturated silicic acid solution will become a monodisperse colloidal silica suspension. The diffusion limited or "fast" aggregation rate constant k_{fast}, is defined by:

$$k_{fast} = \frac{8k_B T}{3\mu} \quad (5)$$

where, k_B is the Boltzmann constant, and μ is the dynamic viscosity of water. k_{fast} reveals the fastest aggregation process as no repulsive effect is considered, i.e. particles aggregate once they collide due to Brownian motion.

The reaction limited, or "slow" aggregation rate constant, k_{slow}, can be considered as k_{fast} divided by the stability ratio W. W can be treated as the inverse of the probability of aggregation. In this case, repulsive effects are taken into account. Therefore, the stability ratio of colloidal silica, W, is defined by (Fuchs 1934):

$$W = \frac{k_{fast}}{k_{slow}} = 2\int_0^\infty \frac{\beta(u)}{(u+2)^2} exp(\frac{V_T(u)}{k_B T})\, du \quad (6)$$

where, $\beta(u)$ is the hydrodynamic correction factor, defined by Eq. 7 below. W quantifies the difficulty of colloidal aggregation. As the silica deposition process on the fracture surface is dominated by the attachment of suspended and deposited silica particles, higher stability can lead to lower deposition rate.

The hydrodynamic correction factor is initially applied to correct the diffusion coefficient due to the effects of viscous drag:

$$D(u) = D_0/\beta(u) \quad (7)$$

where, D_0 is the diffusion coefficient of a particle in an infinitely dilute solution. Therefore, β converges to 1 when the intersphere surface separation approaches infinity, i.e. $H \gg a$.

The expression for the hydrodynamic correction factor in the case of two spherical colloids having the same size is given by (Honig et al. 1971):

$$\beta = \frac{4}{3}\sinh(\alpha)\sum_{n=1}^{\infty}\frac{u(u+1)}{(2u-1)(2u+3)} \cdot [\frac{4\cosh^2(u+\frac{1}{2})\alpha + (2u+1)^2\sinh^2(\alpha)}{2\sinh(2u+1)\alpha - (2u+1)\sinh(2\alpha)} - 1] \quad (8)$$

where α is defined by:

$$\cosh(\alpha) = \frac{u}{2} + 1 \quad (9)$$

The factor can then be numerically approximated to a rational function (Honig, et al. 1971):

$$\beta(u) \approx \frac{6u^2 + 13u + 2}{6u^2 + 4u} \quad (10)$$

At this point, the interaction potential V_T can be predicted by the DLVO theory described previously, the expected stability ratio can then be computed.

It has been shown that DLVO theory can predict the stability of colloids of a range of chemical compositions with reasonable accuracy (Adamczyk and Weroński 1999). However, amorphous silica is an exception (Iler 1979, De Gennes 1987, Healy 1994, Kobayashi et al. 2005).

According to (Iler 1979), the discrepancy is often defined by the following four observations:

1) The point of zero charge (pzc) is usually defined as the pH value at which a particle submerged in a background electrolyte solution shows zero charge on the surface. According to experimental results, the pzc is close to pH = 2, at which the colloidal silica particle is expected to be unstable based on DLVO theory due to the absence of repulsive electrostatic potential. However, in reality silica sols are known to be stable between pH 0 and pH 4.

2) While the concentration of hydrogen ion is decreasing within the range of pH = ~2 to pH = ~6, the degree of surface charge, usually evaluated by surface charge density or zeta-potential, is theoretically predicted and experimentally verified to be increasing. Hence, according to DLVO theory, the stability ratio is expected to be growing, which is in contrast with the reality that it is declining.

3) Although silica colloids show qualitatively DLVO-like behaviour at 6 < pH < 10, the observed stabilities are lower than the predictions by many orders of magnitude.

4) According to DLVO theory, the stability ratio of colloidal silica continuously increases as pH increases from acid to alkaline due to the decreasing concentration of hydrogen ions causing the rise of repulsive electrostatic potential. The difference (the unexpected peak and drop) between the prediction and observations reveals the existence of additional effects not accounted for in DLVO theory.

These four points are qualitatively visualised in Fig. 1 below.

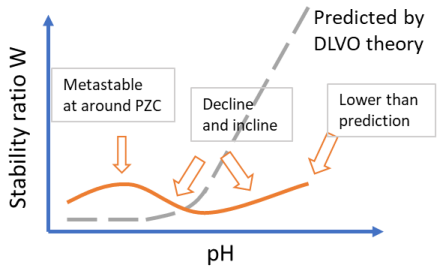

Figure 1: Qualitative comparison between observed and predicted stability of silica nanoparticles.

De Gennes (1987) proposed that these unexpected interaction behaviours are due to a gel or hairy layer, which consists of silicone polymers anchored on the surface of silica particles, as illustrated in Fig. 2.

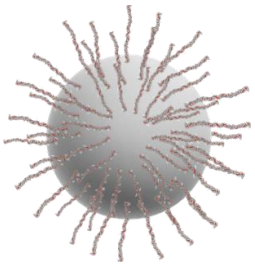

Figure 2: A sketch of a colloidal particle with a hairy layer, the "hairs" being polymer chains of silicone.

Some researchers (De Gennes 1987, Healy 1994) suggested that the major effect of the hairy layer is the extra steric barrier, i.e. the energy barrier caused by overlapping electron clouds.

The effect is to significantly increase the total energy barrier that must be overcome by the colloids to aggregate. De Gennes (1987) published his theory regarding the interaction of particles covered with the hairy layers and assumed that, after the contact of the hairy layers, the polymers compress against each other but do not interdigitate, and concluded that the unique effects are due to the steric interaction.

However, the extra steric barrier will only shift the predicted stability curve above the traditional curve based on the DLVO theory, i.e. it can only predict higher stability than DLVO theory. Experimental observations show the silica colloids also might be less stable than the DLVO predictions at some conditions (Figure 1).

Ohshima (2015) extended De Gennes' model by considering how charged hairy layers would affect the interactions. He suggested (Ohshima 2015) that the particles having charged hairy layers have very different electrostatic behaviours when compared to the particles having no such structures on their surface. Ohshima defined a class of colloid "soft" particles, which are coated by ion-penetrable surface layers of polyelectrolytes.

Ohshima described the compression of the hairy layer, leading to a two-stage soft particle model at the beginning (approach and compression), but soon extended this to include interdigitation of the hairy layer, hence the three-stage soft particle model (Fig. 3). This proved useful in explaining physical problems such as bacterial adhesion, red blood cell aggregation, etc. (Pribush et al. 2007, Hori and Matsumoto 2010).

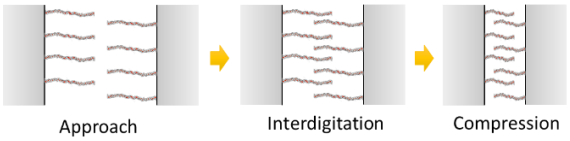

Figure 3: Three stages of aggregating surfaces of two soft particles.

Škvarla (2013) was partially successful in explaining the experimentally observed stability curve by adopting Ohshima's soft-particle model published in 2011. However, since the soft particle model at that time was not fully developed yet – only the approaching process was presented, the discrepancy could not be completely explained. The present work considers whether Ohshima's full model may be applied to the case of silica colloids.

The experimental results used in the present work are reproduced from (Škvarla 2013). Observations were made by measuring the absorbance (at 380, 540, and 800 nm) of a silica-water-KCl suspension system as a function of time under varying chemical conditions (pH = 2.6, 4, 6, and 8; ionic strength = 0.001 to 1 M), revealing the progressing aggregation process. The (50, 150, and 320 nm SEM diameters) silica samples are homogenous nonporous silica having natural hydroxyl silanol groups on the surface, suspended in KCl brines, produced by Bangs Laboratories Inc.

2. OHSHIMA'S THREE-STAGE SOFT PARTICLE MODEL

2.1 Stage I: Approach

To model the electrostatic interaction, it is necessary to solve the Poisson-Boltzmann equations in the range of both inside and outside the hairy layer. For simplicity, one can initially consider two parallel plates 1 and 2 with ion-penetrable hairy layers on the surface, i.e. soft plates. The thicknesses of the layers 1 and 2 are d_1 and d_2 respectively. The two soft plates are separated by a distance H and immersed in a brine having N different ionic species with valence z_i and number density n_i,. The layers 1 and 2 are assumed to be charged at the uniform charge densities ρ_{fix1} and ρ_{fix2} separately, which is defined by $\rho_{fixi} = Z_i e N_i$ where Z_i and N_i are the valence and the number density of the dissociated groups respectively. The coordinate set up is shown in Fig. 4.

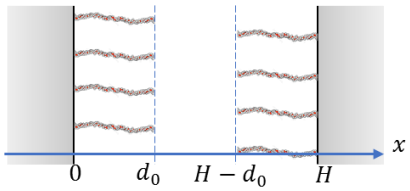

Figure 4: Parallel soft plates showing the different regions: hairy layer 1 ($0 < x < d_0$), solution ($d_0 < x < H - d_0$), and separation distance H.

It is assumed that the electric potential distribution ψ over x can be described using the one-dimensional planar Poisson-Boltzmann equations:

for $-d_1 < x < 0$:

$$\frac{d^2\psi(x)}{dx^2} = -\frac{1}{\varepsilon_r\varepsilon_0}\sum_{i=1}^{N} z_i e n_i \exp\left(-\frac{z_i e\psi(x)}{k_B T}\right) - \frac{\rho_{fix1}}{\varepsilon_r\varepsilon_0} \quad (11)$$

for $0 < x < H$:

$$\frac{d^2\psi(x)}{dx^2} = -\frac{1}{\varepsilon_r\varepsilon_0}\sum_{i=1}^{N} z_i e n_i \exp\left(-\frac{z_i e\psi(x)}{k_B T}\right) \quad (12)$$

for $-d_1 < x < 0$:

$$\frac{d^2\psi(x)}{dx^2} = -\frac{1}{\varepsilon_r\varepsilon_0}\sum_{i=1}^{N} z_i e n_i \exp\left(-\frac{z_i e\psi(x)}{k_B T}\right) - \frac{\rho_{fix2}}{\varepsilon_r\varepsilon_0} \quad (13)$$

However, for simplicity, one can replace the parameters by using a scaled (i.e. non-dimensionalised) forms:

for $d_0 < x < H - d_0$:

$$\frac{d^2y(x)}{dx^2} = \kappa^2 \sinh y \quad (14)$$

for $0 < x < d_0$ and $H - d_0 < x < H$:

$$\frac{d^2y(x)}{dx^2} = \kappa^2(\sinh y - \sinh y_{DON1}) \quad (15)$$

where the scaled electric potential is defined by $y(x) = \frac{ze\psi(x)}{k_B T}$, and the scaled Donnan potential, which is the electric potential due to the distribution of ion species caused by the charged hairy layers, is $y_{DON1} = \frac{ze\psi_{DON1}}{k_B T} = \text{arcsinh}(\frac{ZN_0}{2zn})$.

The following boundary conditions with respect to the left plate are:

$$\left.\frac{dy}{dx}\right|_{x=H/2} = 0 \quad (16)$$

$$\left.\frac{dy}{dx}\right|_{x=d_0^-} = \left.\frac{dy}{dx}\right|_{x=d_0^+} \quad (17)$$

$$y(x = d_0^-) = y(x = d_0^+) \quad (18)$$

$$\left.\frac{dy}{dx}\right|_{x=0^+} = 0 \quad (19)$$

The first boundary condition is due to symmetry, the second is a consequence of assuming the permittivity of the hairy layer and the solution are equal, the combination of the second and third shows that the potential and its gradient are continuous near the layer edge, and the final boundary condition assumes the surface of the particle core is uncharged, i.e. all dissociation sites have been occupied by the polyelectrolyte brushes.

Therefore, the electrostatic force per unit area for $\kappa(H - 2d_0) \geq 1$ and $H \geq 2d_0$ can be found by solving Eq. 14 and 15 using Eq. 16-19:

for $H \geq 2d_0$:

$$P_{pl}(H) = 64nk_BT\tanh^2(y_0/4)\exp[-\kappa(H - 2d_0)] \quad (20)$$

By integrating $P_{pl}(H)$, the electrostatic potential per unit area $V_{pl}(H)$ can be found:

$$\begin{aligned} V_{pl}(H) &= \int_H^\infty P_{pl}(H)\, dH \\ &= \frac{1}{4\varepsilon_r\varepsilon_0\kappa^3}\{\left[\rho_{fix1}\sinh(\kappa d_1) + \rho_{fix2}\sinh(\kappa d_2)\right]^2\left[\coth\left(\frac{\kappa(H + d_1 + d_2)}{2}\right) - 1\right] \\ &\quad - \left[\rho_{fix1}\sinh(\kappa d_1) - \rho_{fix2}\sinh(\kappa d_2)\right]^2\left[1 - \tanh\left(\frac{\kappa(H + d_1 + d_2)}{2}\right)\right]\} \end{aligned} \quad (21)$$

By integrating $V_{pl}(H)$, the electrostatic potential between two spherical colloids 1 and 2 $V_{sp}(H)$ can be found:

$$V_{sp}(H) = \frac{2\pi(a_1 + d_1)(a_2 + d_2)}{(a_1 + d_1) + (a_2 + d_2)}\int_H^\infty V_{pl}(H)\, dH \quad (22)$$

By substituting Eq. 21 to 22 one can find:

$$\begin{aligned} V_{sp}(H) &= \frac{1}{4\varepsilon_r\varepsilon_0\kappa^3}\frac{\pi(a_1 + d_1)(a_2 + d_2)}{a_1 + d_1 + a_2 + d_2}\{\left[\rho_{fix1}\sinh(\kappa d_1) + \rho_{fix2}\sinh(\kappa d_2)\right]^2\ln[\frac{1}{1 - \exp(-\kappa(H + d_1 + d_2))}] \\ &\quad - \left[\rho_{fix1}\sinh(\kappa d_1) - \rho_{fix2}\sinh(\kappa d_2)\right]^2\ln[1 + \exp(-\kappa(H + d_1 + d_2))]\} \end{aligned} \quad (23)$$

2.2 Stage II: Interdigitation

Next, the case of interdigitation, as shown in Figure 5, is considered. The coordinates set up is shown below.

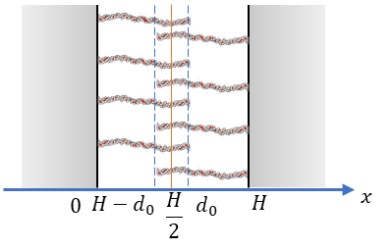

Figure 5: Parallel soft plates showing the different regions: hairy layer 1 ($0 < x < H - d_0$), interdigitation zone ($H - d_0 < x < d_0$), and separation distance H.

As shown in Fig. 5, the layers within the range $0 < x < H - d_0$ and $d_0 < x < H$ are undisturbed, and in $H - d_0 < x < d_0$ are interdigitating. For this case, the assumption of uniformly distributed dissociated groups remains. Therefore, the number density of ionised groups in $0 < x < H - d_0$ and $d_0 < x < H$ is still N_0, and in $H - d_0 < x < d_0$ shall be

$2N_0$. It is assumed that the electric potential in the case of interdigitation follows the Poisson-Boltzmann equations below:

for $0 < x < H - d_0$ and $d_0 < x < H$:

$$\frac{d^2y(x)}{dx^2} = \kappa^2(\sinh y - \sinh y_{DON1}) \tag{24}$$

for $H - d_0 < x < d_0$:

$$\frac{d^2y(x)}{dx^2} = \kappa^2(\sinh y - \sinh y_{DON2}) \tag{25}$$

where y_{DON1} and y_{DON2} are the scaled Donnan potentials in the regions of undisturbed and interdigitation respectively, which are defined by $\sinh y_{DON1} = \frac{zN_0}{2zn}$, $\sinh y_{DON2} = \frac{zN_0}{zn}$.

The following boundary conditions with respect to the left plate are:

$$\left.\frac{dy}{dx}\right|_{x=h/2} = 0 \tag{26}$$

$$\left.\frac{dy}{dx}\right|_{x=h-d_0^-} = \left.\frac{dy}{dx}\right|_{x=h-d_0^+} \tag{27}$$

$$y(x = h - d_0^-) = y(x = h - d_0^+) \tag{28}$$

$$\left.\frac{dy}{dx}\right|_{x=0^+} = 0 \tag{29}$$

With the boundary condition above (Eq. 26-29), Eq. 24 and 25 can be solved, and the electrostatic force per unit area can be found:

for $d_0 < H < 2d_0$:

$$\begin{aligned} &P_{pl}(H) \\ &= 4nk_BT\left\{\sinh^2\left[\frac{y_{DON2}}{2}\right.\right. \\ &- \frac{y_{DON2} - y_{DON1}}{2G(H)}\sinh\big(\kappa_1(H \\ &- d_0)\big)\cosh\left[\kappa_2\left(\frac{H}{2} - d_0\right)\right]\Big] \\ &- \frac{1}{4}\left(\frac{\kappa_2}{\kappa}\right)^2\left(\frac{y_{DON2} - y_{DON1}}{G(H)}\right)^2\sinh^2\left[\kappa_2\left(\frac{H}{2}\right.\right. \\ &\left.\left.\left. - d_0\right)\right]\right\} \end{aligned} \tag{30}$$

where $G(H)$ is defined by:

$$\begin{aligned} G(H) = \sinh\big(\kappa_1(H - d_0)\big)\cosh\left[\kappa_2\left(\frac{H}{2} - d_0\right)\right] \\ - \left(\frac{\kappa_2}{\kappa_1}\right)\cosh\big(\kappa_1(H \\ - d_0)\big)\sinh\left[\kappa_2\left(\frac{H}{2} - d_0\right)\right] \end{aligned} \tag{31}$$

where $\kappa_1 = \kappa\sqrt{\cosh(y_{DON1})}$ and $\kappa_2 = \kappa\sqrt{\cosh(y_{DON2})}$ physically mean the Debye-Hückel parameters in the undisturbed and interdigitation regions respectively.

The electrostatic interaction potential between the spherical particles can be found by following the same method described in Eq. 21-23, or by solving numerically.

2.3 Stage III: Compression

Now, consider the third stage for the two-stage model (shown in the figure below): after the hairy layers interdigitate to a distance H_c, the polymer chains start to compress, as shown in Fig. 6 below.

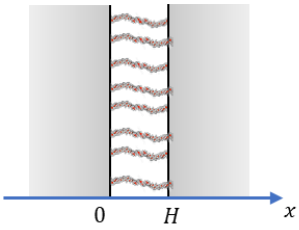

Figure 5: Parallel soft plates showing the compression stage.

For simplicity, only the case of full interdigitation is considered in this work, i.e. the compression stage starts when the brushes are completely interdigitated ($H_c = d_0$).

The separation distance can then be expressed by H = d ≤ d_0.

Previously, it was assumed that the layer is uniformly charged and the charge density (ρ_{fix1} and ρ_{fix2}) is a constant. However, in this case, it is a function of H, i.e. increasing while compressing. The assumption of uniformly distributed charged groups remains. For simplicity, it is assumed that $N_1 = N_2 = 2N_0$, i.e. the subscript "0" means "undisturbed". Therefore, the number density of the ionised groups N′ in this case can be related to the undisturbed number density $2N_0$:

$$N'\frac{\mathrm{H}}{2} = N_0 d_0 \tag{32}$$

Since the potential within the compressed layers is constant (both layers are uniformly charged) and depends on the separation distance H but not on the location x, it is assumed that the scaled electric potential $y(x) = ze\psi(x)/k_BT$ obeys the following Poisson-Boltzmann equation:

for $0 < x \leq 2d_0$:

$$\frac{d^2y(x)}{dx^2} = \kappa^2\left[\sinh y - \frac{ZN'}{2zn}\right] = 0 \tag{33}$$

i.e. the electric potential is equal to the Donnan potential $\psi_{DON}'(H)$ for this case everywhere. Therefore, the formula containing the scaled Donnan potential y_{DON}' in this case can be derived:

$$\sinh[y_{DON}'(H)] = \frac{ZN'}{2zn} = \frac{ZN_0d_0}{znH} \tag{34}$$

By solving, one can find the electrostatic force per unit area:

for $0 < H \leq 2d_0$:

$$P_{pl}(H) = 2nk_BT\left[\sqrt{\left(\frac{ZN_0d_0}{znH}\right)^2 + 1} - 1\right] \tag{35}$$

The related potential can be found by following the approach described previously (Eq. 21-23).

The interaction between soft particles can be modelled using this three-stage approach. Compared to the classic model, the

charged hairy layer with finite thickness (d_0) can provide a stronger but not excessively repulsive potential, like the steric barrier.

When the two particles aggregate, the separation distance H is called the capture distance H_c. In the frame of DLVO theory, it is usually assumed to be 0, i.e. one particle captures the other once their separation distance becomes 0 ($H_c = 0$).

In contrast, different stages in the soft particle model can be considered by positing different capture distances. To find the stability, the integral in Eq. 6 shall be performed from infinity to the assumed capture distance H_c instead of to 0. Therefore, there are three cases to be considered.

1. The capture distance is $2d_0$ (i.e. $H_c = 2d_0$). The two particles are attached once the hairy layers touch each other, i.e. only Stage I (approach) is taken into account;

2. The capture distance is between d_0 and $2d_0$ (i.e. $d_0 \leq H_c < 2d_0$). The two particles are attached till the hairy layers become interdigitated, i.e. both Stage I and II (approach and interdigitation) are considered;

3. The capture distance is less than d_0 ($H_c < d_0$). The two particles aggregate till the hairy layers are compressed, i.e. all three stages (approach, interdigitation, and compression) are applied.

Note that the thickness of hairy layers d_0 only limits the bounds of H_c for the three cases.

When the background chemical (pH and ionic strength) conditions are given, the surface charge can be found. The approach taken in this study is to adjust d_0 until the predicted stability matches the observation under the same conditions. If such a match can be found across a range of pH, it is inferred that the soft particle model better represents the physics of silica colloid interaction than does the DLVO theory. The fitting process is summarised in Fig. 6 below:

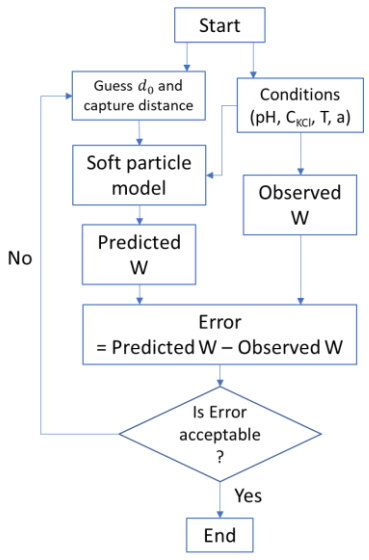

Figure 6: The workflow of the fitting process. d_0 is the only free parameter, and all other values are taken from the reported experimental conditions. The observed stability can be fitted almost exactly (All Errors are less than 5% of observed *W*) by giving a separate value of d_0 for each experiment. Recall that *a* represents the radius of the particle (hairy layer excluded).

3. FITTING RESULTS AND DISCUSSION

The complete set of inputs and fitting results is included in the appendix. The only free parameter is d_0, which is assumed to be a function of pH, c_{KCl}, and particle size a. The values of d_0 obtained are plotted in Fig. 7.

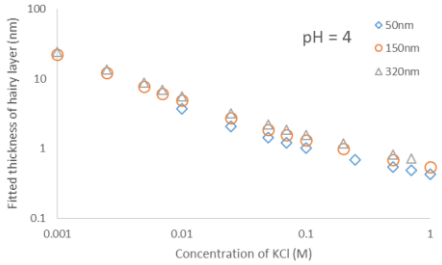

(a)

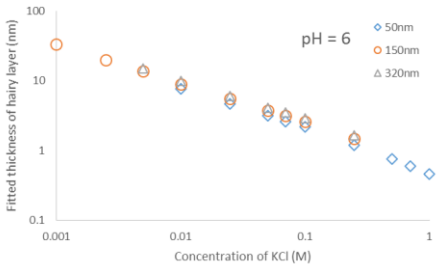

(b)

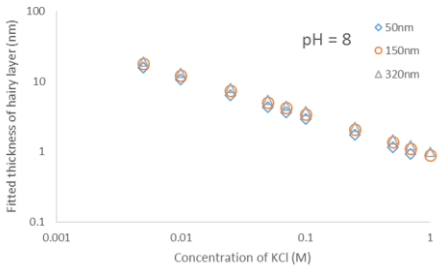

(c)

Figure 7: Fitted hairy layer thickness as a function of KCl concentration and pH.

A systematic variation of the fitted d_0 values with c_{KCl}, a and pH is seen, suggestive of a physical relationship. d_0 is seen to be strongly dependent, and nearly linear with, c_{KCl}, only weakly dependent on particle size a, and modestly increasing as pH rises.

By assuming that the capture distance is $2d_0$ (i.e. only Stage I is considered), which physically means that the particles are successfully linked once the hairy layers from two particles collide as shown in Fig. 8 below, the fitting results are good enough to conclude that Ohshima's soft particle model is valid to explain the unexpected interactions between the colloidal silica at least in the range of pH = 4, 6, and 8, c_{KCl} = 0.001-1 M.

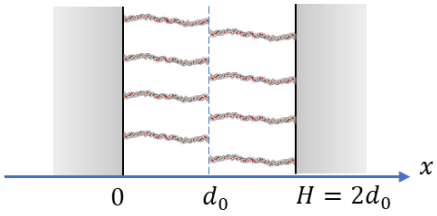

Figure 8: Two soft particles aggregate once two hairy layers collide. This is equivalent to Fig. 4 when the separation distance H is equal to $2d_0$. At this moment, $H = H_c = 2d_0$.

As d_0 is fitted to match the observed stability, the observed stability behaviour is directly reproduced by this new model (Fig. 9). Hairy layer thickness varies with pH, and thus so does repulsive electrostatic potential, which permits variations in stability that are not predicted by the classic DLVO theory.

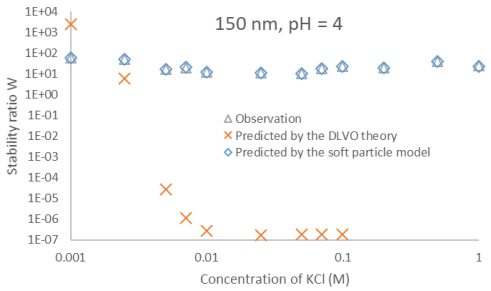

Figure 9: Comparison between the observed and the predicted (by the DLVO theory and the soft particle model) stability as a function of c_{KCl} for 150 nm in diameter silica particles at pH = 4, and 25 ℃.

4. INTERPRETATION OF THE VARYING HAIRY LAYER THICKNESS

According to Fig. 7, it can be concluded that the variation in d_0 is dominated by pH and the concentration of KCl (or ionic strength of the background electrolyte if the effects of varying the salt species are negligible). Particle size has minor effects as well. The results seem reasonable, since the more favourable the conditions are to silica polymerisation (i.e. high pH and low ionic strength), the thicker the hairy layers are expected to be.

By ignoring the effects of particle size, a linear correlation between log d_0 and log c_{KCl} can be fitted:

at pH = 4 ($R^2 = 0.97$),

$$\log d_0 = -0.5535 \log c_{KCl} - 0.3957 \qquad (36)$$

at pH = 6 ($R^2 = 0.98$),

$$\log d_0 = -0.6032 \log c_{KCl} - 0.2403 \qquad (37)$$

at pH = 8 ($R^2 = 0.99$),

$$\log d_0 = -0.5698 \log c_{KCl} - 0.1062 \qquad (38)$$

Eqs. 36-38 may be safely applied to estimate the thickness of the hairy layers at pH = 4, 6, and 8 and $c_{KCl} = 0.001 - 1$M at 25℃. If it is reasonable to ignore the errors introduced by different salts, c_{KCl} can be directly replaced with the ionic strength I, which is in the range of 0.001-1 M as well, and this range of I may cover typical geothermal conditions (about 0.07 M in New Zealand fields, dominated by the concentration of sodium chloride).

5. CONCLUSION

Inspired by the work of Škvarla (2013), Ohshima's latest soft particle model (Ohshima 2015) is shown to explain the unexpected interaction behaviours at pH = 4, 6, and 8 and $c_{KCl} = 0.001 - 1$M at 25℃, which may offer a better understanding of the mechanisms for silica particle attachment and silica scaling, at least at room temperature. Further experimental studies may be of interest to investigate the interactions between silica particles and silica coated plates at high temperature in the frame of soft particle model.

REFERENCES

Adamczyk, Z. and P. Weroński (1999). "Application of the DLVO theory for particle deposition problems." Advances in colloid and interface science 83(1-3): 137-226.

Brown, K. (2011). Thermodynamics and kinetics of silica scaling. Proceedings of International Workshop on Mineral Scaling.

De Gennes, P. (1987). "Polymers at an interface; a simplified view." Advances in colloid and interface science 27(3-4): 189-209.

Deraguin, B. and L. Landau (1941). "Theory of the stability of strongly charged lyophobic sols and of the adhesion of strongly charged particles in solution of electrolytes." Acta Physicochim: USSR 14: 633-662.

Derjaguin, B. (1940). "On the repulsive forces between charged colloid particles and on the theory of slow coagulation and stability of lyophobe sols." Transactions of the Faraday Society 35: 203-215.

Fuchs, N. (1934). "Zur theorie der koagulation." Zeitschrift für Physikalische Chemie 171(1): 199-208.

Hamaker, H. (1937). "The London—van der Waals attraction between spherical particles." physica 4(10): 1058-1072.

Healy, T. W. (1994). "Stability of aqueous silica sols." Advances in Chemistry Series 234: 147-147.

Honig, E., et al. (1971). "Effect of hydrodynamic interaction on the coagulation rate of hydrophobic colloids." Journal of Colloid and Interface Science 36(1): 97-109.

Hori, K. and S. Matsumoto (2010). "Bacterial adhesion: from mechanism to control." Biochemical Engineering Journal 48(3): 424-434.

Iler, R. K. (1979). "Chemistry of Silica--Solubility, Polymerization, Colloid and Surface Properties, and Biochemistry."

Kobayashi, M., et al. (2005). "Aggregation and charging of colloidal silica particles: effect of particle size." Langmuir 21(13): 5761-5769.

London, F. (1937). "The general theory of molecular forces." Transactions of the Faraday Society 33: 8b-26.

Ohshima, H. (2015). "Electrostatic interaction of soft particles." Advances in colloid and interface science 226: 2-16.

Pribush, A., et al. (2007). "The mechanism of the dextran-induced red blood cell aggregation." European Biophysics Journal 36(2): 85-94.

Škvarla, J. i. (2013). "Quantitative interpretation of anomalous coagulation behavior of colloidal silica using a swellable polyelectrolyte gel model of electrical double layer." Langmuir 29(28): 8809-8824.

Sonnefeld, J. (1995). "Surface charge density on spherical silica particles in aqueous alkali chloride solutions." Colloid and polymer science 273(10): 932-938.

Verwey, E. J. W. and J. T. G. Overbeek (1955). "Theory of the stability of lyophobic colloids." Journal of Colloid Science 10(2): 224-225.

Weres, O., et al. (1981). "Kinetics of silica polymerization." Journal of Colloid and Interface Science 84(2): 379-40

APPENDIX

Table A1: Stability fitting results: d is the average diameter of silica particle samples; I is the ionic strength, which is equal to the concentration of KCl in this case; $-\sigma_0$ is the surface charge density reproduced from (Škvarla 2013) and estimated by following (Sonnefeld 1995) if the experimental data is not presented; W is the observed stability; W_{DLVO} is the estimated stability using the DLVO theory (missing data due to the absent of the corresponding zeta-potential); W' is the fitted stability using the soft particle model; d_0 is the fitted thickness of hairy layers.

		pH = 4											
		d = 50nm				d = 150nm				d = 320nm			
I(M)	$-\sigma_0$ (mC m^{-2})	W	W_{DLVO}	W'	d_0(nm)	W	W_{DLVO}	W'	d_0(nm)	W	W_{DLVO}	W'	d_0(nm)
0.001	1.39	-				58.3	2.41E+03	58.12	22.29	220.0	8.10E+15	219.52	24.38
0.0025	1.42	-				49.6	5.83	49.84	12.09	100.0	2.26E+10	100.43	13.50
0.005	1.48	-				16.1	2.69E-05	16.04	7.69	22.0	0.08	22.03	8.71
0.007	1.51	-				20.0	1.16E-06	20.10	6.12	17.0	6.74E-05	17.08	7.00
0.01	1.57	8000.0	6.63E-08	7.91E+03	3.72	12.0	2.70E-07	11.93	4.87	12.0	1.13E-06	11.88	5.59
0.025	1.89	1010.0	5.48E-08	1.03E+03	2.08	11.0	1.77E-07	10.88	2.75	8.0	3.99E-07	7.98	3.20
0.05	2.43	110.0	5.59E-08	113.54	1.42	10.0	1.81E-07	10.17	1.86	5.1	4.08E-07	5.07	2.19
0.07	2.85	105.0	5.60E-08	102.86	1.19	18.0	1.81E-07	17.48	1.56	3.6	4.06E-07	3.53	1.85
0.1	3.49	110.0	5.70E-08	110.72	1.01	22.0	1.84E-07	22.85	1.31	5.4	4.14E-07	5.47	1.55
0.2	5.87	-				20.0		19.89	1.00	4.0		4.06	1.17
0.25	6.69	140.0		149.36	0.69	-				-			
0.5	12.02	500.0		541.76	0.54	38.0		38.16	0.69	5.1		5.27	0.81
0.7	16.28	600.0		626.80	0.48	-				9.5		9.77	0.71
1	22.67	700.0		731.57	0.43	25.0		23.52	0.55	-			
		pH = 6											
		d = 50nm				d = 150nm				d = 320nm			
I(M)	$-\sigma_0$ (mC m^{-2})	W	W_{DLVO}	W'	d_0(nm)	W	W_{DLVO}	W'	d_0(nm)	W	W_{DLVO}	W'	d_0(nm)
0.001	6.53	-				161.3	1.10E+19	161.73	33.02	-			
0.0025	8.58	-				128.8	2.56E+13	128.38	19.80	-			
0.005	11.30	-				103.5	6.04E+09	104.15	13.69	230.0	4.99E+29	229.95	14.82
0.01	11.90	55000.0	3.34E-06	5.51E+04	7.63	88.2	0.31	88.74	8.985	100.0	5.25E+07	99.84	9.83
0.025	17.06	23000.0	3.38E-08	2.25E+04	4.65	35.9	0.0061	35.70	5.542	110.0	1.29E+04	109.99	6.06
0.05	20.80	20000.0	3.05E-08	2.00E+04	3.13	27.4	7.05E-05	26.90	3.769	80.0	0.9961	78.70	4.13
0.07	23.20	5000.0	3.05E-08	5.07E+03	2.61	16.4	6.75E-06	16.40	3.142	5.0	0.0063	5.11	3.49
0.1	26.50	300.0	3.05E-08	289.36	2.18	5.2	1.11E-06	5.26	2.612	4.5	9.93E-05	4.44	2.89
0.25	27.05	250.0		257.21	1.20	3.7		3.67	1.467	1.3		1.28	1.65
0.5	27.20	280.0		306.21	0.75	-				-			
0.7	27.21	300.0		326.44	0.60	-				-			
1	27.22	390.0		371.22	0.46	-				-			
		pH = 8											
		d = 50nm				d = 150nm				d = 320nm			
I(M)	$-\sigma_0$ (mC m^{-2})	W	W_{DLVO}	W'	d_0(nm)	W	W_{DLVO}	W'	d_0(nm)	W	W_{DLVO}	W'	d_0(nm)
0.005	52.60	4.00E+05	5.61	3.99E+05	15.89	348.8	2.36E+18	347.39	17.90	205.0	1.16E+48	204.83	19.21
0.01	58.20	3.00E+05	5.00E-05	3.01E+05	10.68	187.5	1.33E+03	187.81	12.19	105.0	3.15E+15	105.09	13.14
0.025	71.60	1.95E+05	2.59E-06	1.96E+05	6.39	156.3	0.19	157.00	7.38	100.0	2.04E+07	99.26	7.99
0.05	82.50	2.50E+04	2.76E-07	2.56E+04	4.35	123.5	1.33E-04	122.61	5.03	90.0	3.93	89.37	5.46
0.07	88.20	1.40E+04	1.47E-07	1.39E+04	3.61	68.4	1.12E-05	69.13	4.18	60.0	0.02	61.12	4.54
0.1	95.20	8000.0	2.03E-07	8.27E+03	2.95	74.6	4.97E-05	77.77	3.43	18.0	0.54	18.25	3.75
0.25	103.92	1010.0		963.39	1.74	7.1		7.05	2.05	1.3		1.26	2.25
0.5	117.20	600.0		624.16	1.16	5.2		5.15	1.37	1.4		1.43	1.51
0.7	117.20	750.0		751.84	0.94	6.0		6.03	1.11	1.8		1.87	1.23
1	117.21	-				7.0		7.54	0.89	2.2		2.12	0.99